

Supplementary Information (SI) for

**Interfacial triplet confinement for achieving efficient
solution-processed deep-blue and white electrophosphorescent
devices with the underestimated poly(N-vinylcarbazole) as host**

Baohua Zhang,^a Lihui Liu,^{ac} Guiping Tan,^{bd} Bing Yao,^a Cheuk-Lam Ho,^b Shumeng Wang,^{ac} Junqiao Ding,^a Zhiyuan Xie,^{*a} Wai-Yeung Wong,^{*b} and Lixiang Wang^a

^a State Key Laboratory of Polymer Physics and Chemistry, Changchun Institute of Applied Chemistry, Chinese Academy of Sciences, Changchun 130022, P. R. China, E-mail: xiezy_n@ciac.jl.cn

^b Institute of Molecular Functional Materials (Areas of Excellence Scheme, University Grants Committee, Hong Kong) and Department of Chemistry and Institute of Advanced Materials, Hong Kong Baptist University, Waterloo Road, Hong Kong, P. R. China,

E-mail: rwywong@hkbu.edu.hk

^c University of Chinese Academy of Sciences, Beijing 100039, P. R. China

^d College of Chemistry and Environmental Engineering, Dongguan University of Technology, Dongguan 523808, P. R. China

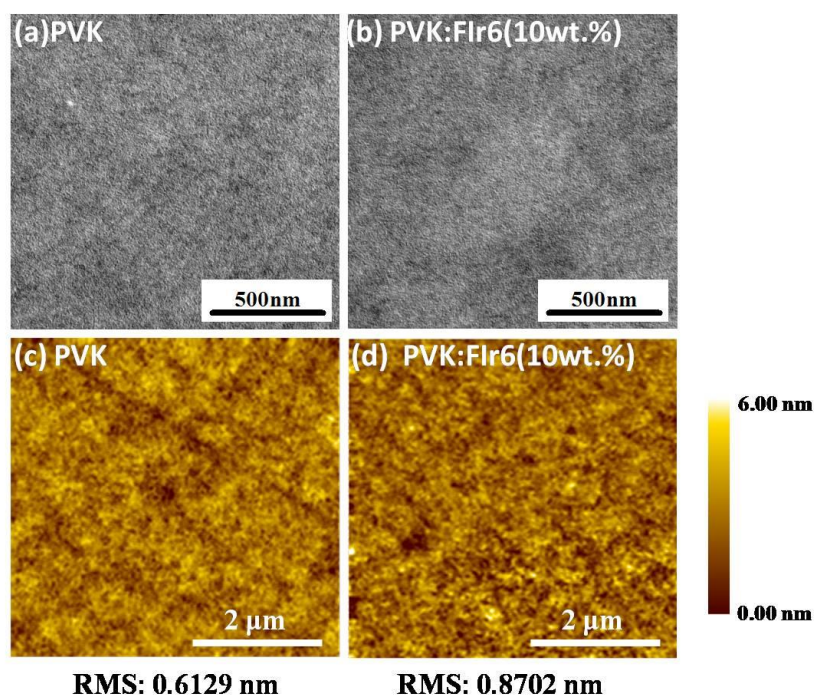


Figure S1. TEM and AFM morphologies of PVK and PVK:Fir6 (10 wt.%) films. As shown, the spin-coated PVK:Fir6 film with a doping ratio of 10 wt.% exhibits comparable film-forming behaviors to the pure PVK film, which demonstrates the excellent miscibility between Fir6 dopant and PVK host in the spin-coated films.

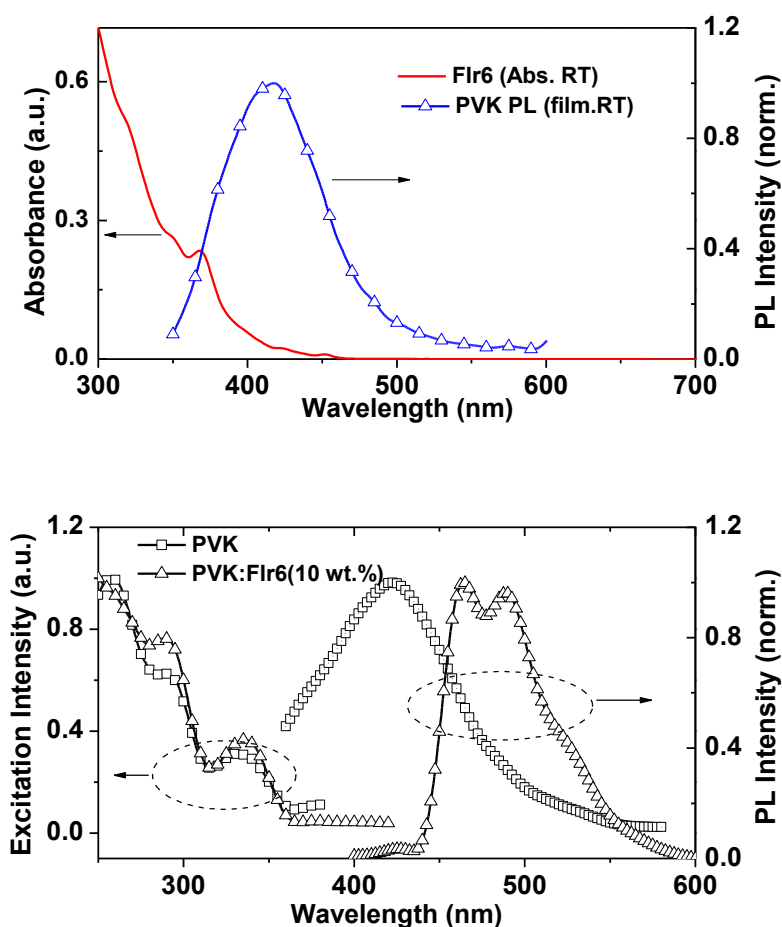


Figure S2. Photophysical behaviors of PVK, FIr6 and PVK:FIr6 (10 wt.%) emissive layer film. (top) PL spectra of PVK film and absorption spectra of FIr6; (bottom) Excitation and PL spectra of PVK and PVK:FIr6(10 wt.%) films (the excitation spectra are recorded at 420 nm for PVK and 460 nm for PVK:FIr6 film samples, respectively).

From top figure, a large spectral overlap between the PL emission of PVK film (peak located at ca. 420 nm) and the absorption bands of both 1MLCT and 3MLCT states of FIr6 exists, which fulfills the requirements of efficient Förster and Dexter energy transfer.[S1] From bottom figure, we note that PL emission of PVK is nearly completely quenched and the FIr6 phosphorescent emission is dominated for the overall PL spectra, indicating the energy transfer from PVK to FIr6 is actually efficient in PVK:FIr6 (10wt.%) film. Besides, the excitation spectra of FIr6 emission (peak located at 460 nm) is basically identical to that of PVK host emission (peak located at 420 nm) and different from the absorption spectra of FIr6 phosphors.

Accordingly, the energy transfer from PVK host rather than the self-absorption of FIr6 dopant is the dominant origin accounting for the FIr6 phosphorescent PL emission in the PVK:FIr6 (10wt.%) film.

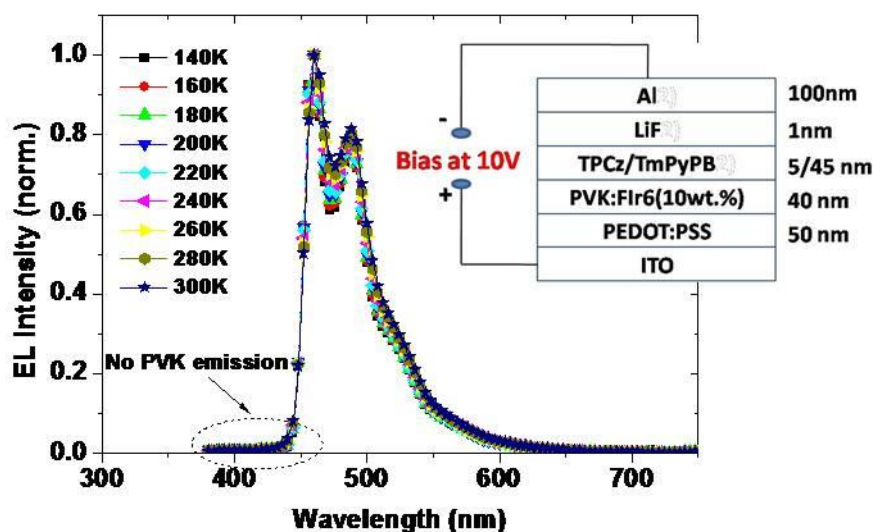


Figure S3. EL spectra of the PVK:Fir6 (10 wt.%) PhOLEDs at a constant bias voltage of 10 V under a range of ambient temperatures. As mentioned,[S2, S3] the temperature-dependent EL spectral measurement of the phosphorescent dye-doped OLEDs is a useful way to confirm the effectiveness of energy transfer process from host to dopant in real devices since the possible existing emission of host material can be effectively magnified at low temperatures owing to the restrained nonradiative pathways of emissive species. As shown in Figure S3, no PVK emission is observed over the wide range of temperatures, indicating that the energy transfer process from host PVK to Fir6 in the real device is basically efficient.

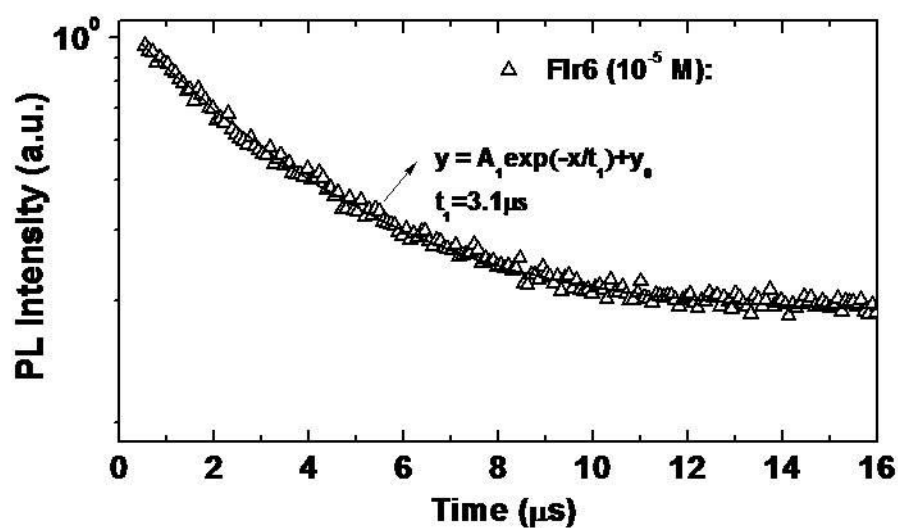


Figure S4. PL decay transient of FIr6 in 10^{-5} M chlorobenzene solution at room temperature. The solid line is mono-exponential fit to the data, achieving the intrinsic lifetime of FIr6 dopant under PL excitation. As depicted, the intrinsic PL transient process is monoexponential and the calculated lifetime of FIr6 is *ca.* 3.1 μs . Accordingly, for the host:FIr6 films (host: PVK, SPPO13, TmPyPB and TPCz), the fast component (corresponding to a short lifetime value) of the fitted bi-exponential behaviors reflects the back energy transfer from FIr6 to the triplet states of the host.^[S4]

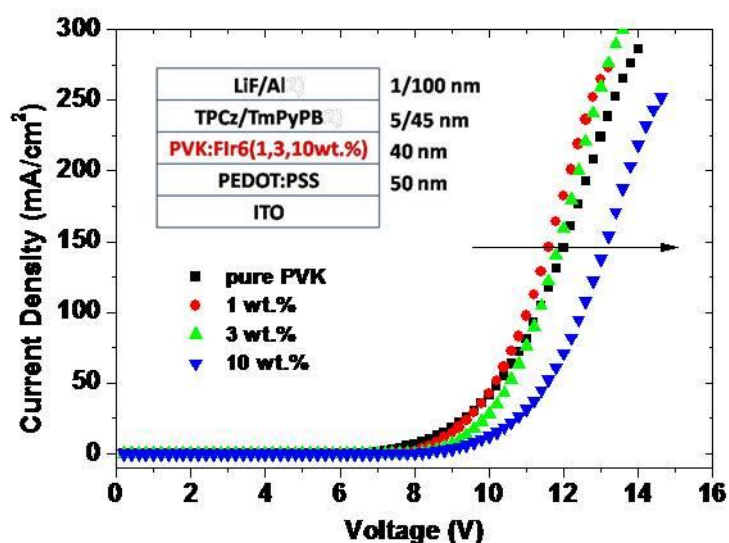


Figure S5. Current-voltage (J - V) characteristics of the PVK:FIr6-based devices with different FIr6 concentration. It can be seen that, at a high doping concentration of FIr6 (10 wt.%), the current is lowered compared to that of the pure PVK control device, verifying the charge-trapping effect of FIr6 in the emissive layer.^[S5] It is proposed that the electron charge trapping effect of FIr6 is responsible for this phenomenon based on the energy level diagram shown in Fig.1. It is concluded that both the energy transfer from PVK to FIr6 and the charge trapping effect of FIr6 dopant are responsible for the final blue EL emission in the device.

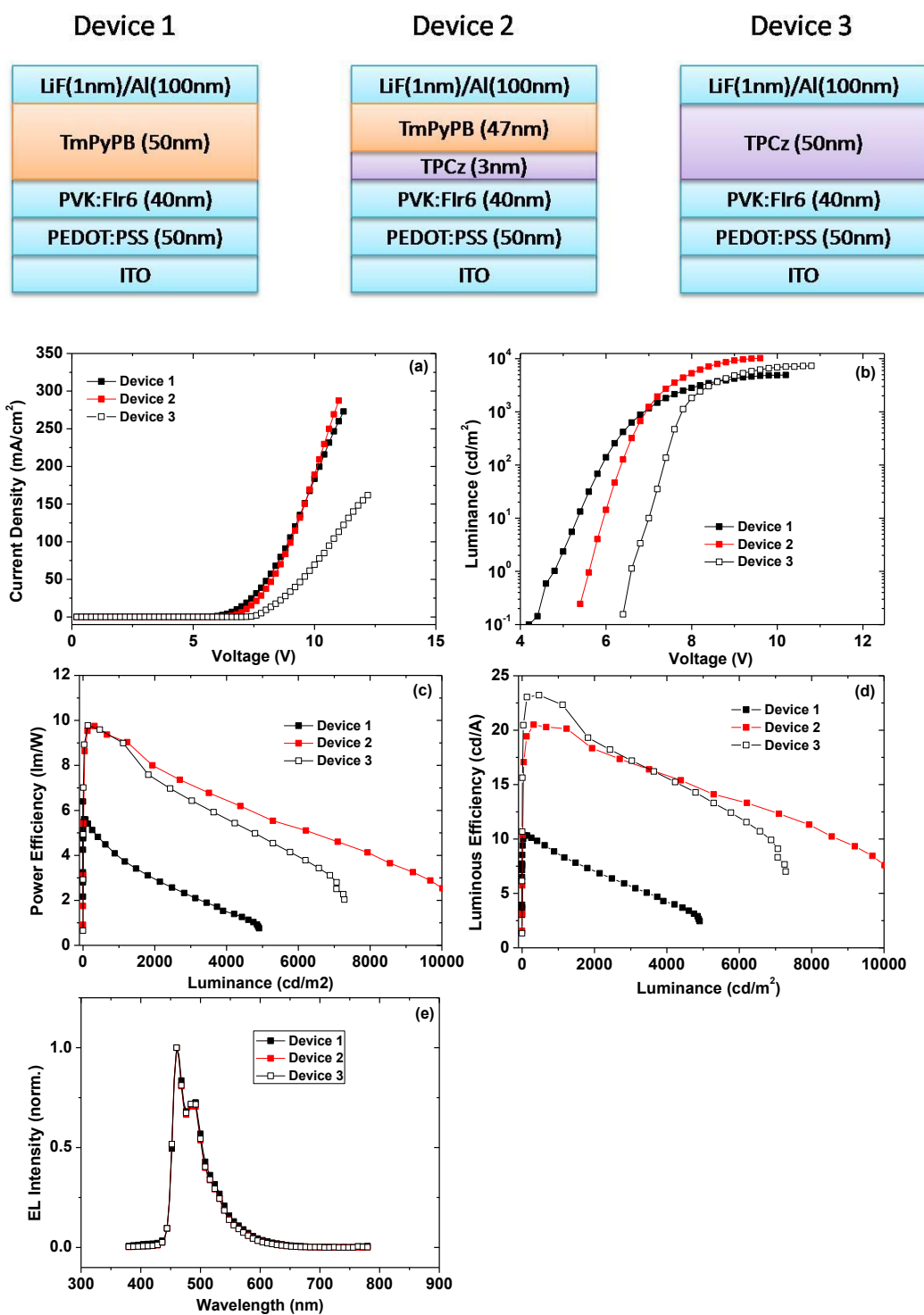


Figure S6. Device characteristic comparisons of the PVK:Flr6-based devices with varied IL/ETL structures of TmPyPB(50nm), TPCz(3nm)/TmPyPB(47nm) and TPCz(50nm) (that is Device 1, 2, and 3), respectively.

As an example, device 1, 2 and 3 in together (see Figure S6, top) illustrated the paramount importance of triplet confinement at the EML/EIL interface rather than the

properties of charge carrier mobility and/or the charge carrier distributions in the EML with ETL materials of TPCz and TmPyPB for achieving ultra-highly efficient PVK-FIr6 based deep-blue devices. For device 2, an ultra-thin 3-nm-thick TPCz was deliberately used as IL to solely function as the exciton confining layer and basically do not influence the charge transport property of the device. It is true and confirmed by the experimental results (Figure S6a). As shown, the device current of device 1 and 2 is really comparable. However, device 2 shows a distinctly higher efficiencies than that of device 1 with pure TmPyPB as IL and ETL(that is peak luminous efficiencies of device 2 and 1 are 20.5 cd/A and 10.5 cd/A, respectively). Accordingly, it is concluded that it is the different interfacial triplet confinement capability at the EML/IL interface that determines the final efficiencies achieved. Besides, in spite of a distinct difference in device current achieved, luminous efficiency of device 2 is basically comparable to that of device 3 with pure low electron transport TPCz as both IL and ETL, which further suggests that the difference in charge carrier mobility between TPCz and TmPyPB is not the main origin for the high luminous efficiency achieved with high triplet level TPCz as IL.

Besides, as shown in Fig. S6e, all these devices shows a comparable EL spectra characteristics (in details, basically the same relative intensity between EL peak at 459 nm and EL shoulder peak at 489 nm). Therefore, interference effects have a negligible influence on the diverse efficiencies achieved for these devices. It is concluded that the exciton recombination profiles within these devices are basically the same, confirming the different IL used in these devices do not obviously affect charge carrier distributions in the active layer.^[S6]

Up to now, the above demonstration confirms that interfacial triplet confinement of TPCz plays the key role in achieving highly efficient deep-blue devices and the other possible factors including charge carrier mobility and the charge carrier distribution (thus exciton formation profiles)within the EML play minor roles. However, we should further mentioned that the usage of high electron mobility of TmPyPB is important for achieving high device power efficiency in the structures of TPCz(as IL)/TmPyPB(as ETL). As shown in Fig. S6b and Fig. S6c, device 2 shows

the lower driving voltage and higher power efficiency than that of device 3 owing to the incorporation of TmPyPB as ETL.

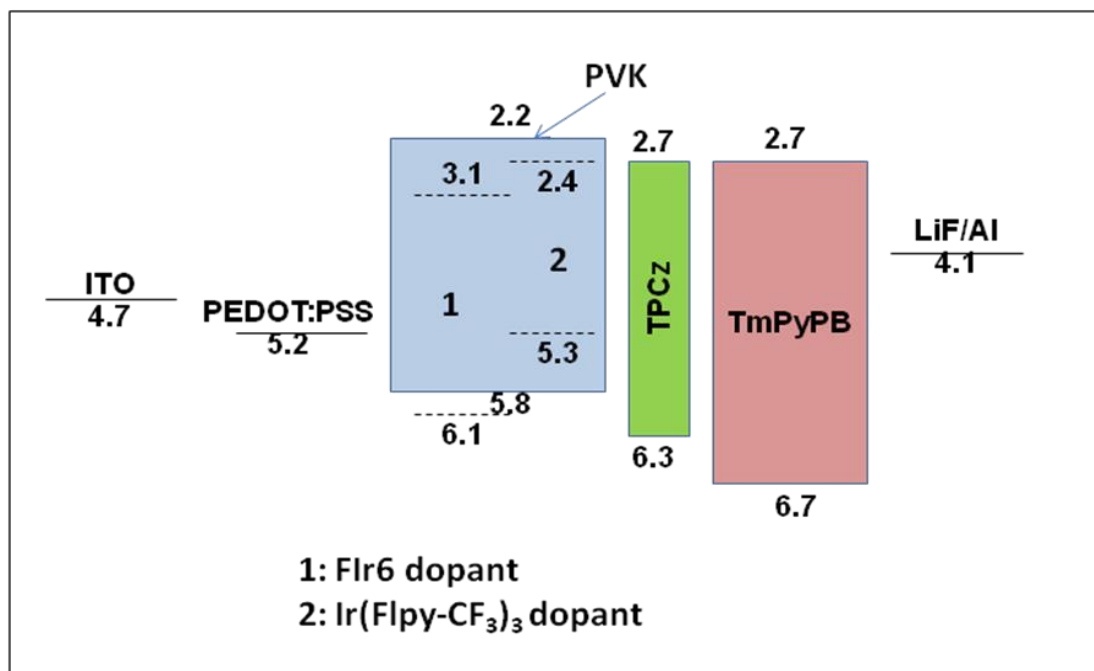


Figure S7. Energy level diagram of the solution-processed white PhOLEDs with a structure of ITO/PEDOT:PSS (50 nm)/PVK:Flr6:Ir(Flpy-CF₃)₃ (90:10:x, w/w/w) (40 nm)/TPCz (8 nm)/TmPyPB (42 nm)/LiF (1 nm)/Al (100 nm).

Table S1. Summary of the reported solution-processed deep-blue PhOLEDs in comparison to our work.

| Ref. | EQE (%) | η_p [lm W^{-1}] | Device Structure |
|--------------------|---|-------------------------------------|--|
| | at 100/1000/5000 cd m^{-2} | at 100/1000/5000 cd m^{-2} | |
| S7 | 1.48/-/- | -/-/- | ITO/PEDOT/PVK:FIr6/TPBI/CsF/Al |
| S8 | 6.3 ^[a] /5.7/- | 6.2/-/- | ITO/PEDOT/P-TAZSiTPA:FIr6/TmPyPB/TPBI/LiF/Al |
| S9 | 6.8 ^[a] /-/- | 4.9/-/- | ITO/PEDOT/BTCC-36:FIr6/TAZ/Cs2CO3/Al |
| S10 ^[b] | 18.9/15.1 ^[c] / ^[d] | -/-/- | ITO/PEDOT/PVK/mCPPO1:FCNIrpic/TSPO1/LiF/Al |
| This work | 16.8/16.1/13.0 | 18.0/15.1/10.5 | ITO/PEDOT/PVK:FIr6/TPCz/TmPyPB/LiF/Al |

[a] peak values; [b]: using deep-blue FCNIrpic dopant; [c] at 500 cd m^{-2} ; [d] max. luminance < 5000 cd m^{-2} .

Table S2. Comparison of the device performance of the reported solution-processed white PhOLEDs with FIrpic or FIr6 as blue phosphor (forward-viewing performance).

| Ref. | Blue phosphor | EQE (%) | η_p [lm W^{-1}] at | C.I.E ^[c] | CRI ^[c] |
|--------------------------------|-----------------|----------------------------------|------------------------------------|----------------------|--------------------|
| | | 100/1000/5000 cd m^{-2} | 100/1000/5000 cd m^{-2} | | |
| S11 ^[a] | Sky-blue FIrpic | 18.3/15.0/10.3 | 33.1/21.4/11.3 | 0.39, 0.42 | 65 |
| S11 ^[b] | Sky-blue FIrpic | 26.0/16.4/9.6 | 47.6/23.3/10.0 | 0.38, 0.43 | 62 |
| This work^[a] | deep-blue FIr6 | 16.9/16.4/13.1 | 24.9/20.7/14.2 | 0.36, 0.38 | 68 |

[a] with PEDOT:PSS AI 4083 as HIL; [b] with PEDOT:PSS CH8000 as HIL; [c] at 1000 cd m^{-2} .

References

- [S1] a) R. Forster, *Organic Charge Transfer Complexes*, Academic Press Inc., 1969;
b) D. L. Dexter, *J. Chem. Phys.* **1953**, *21*, 836.
- [S2] Q. Wang, J. Ding, D. Ma, Y. Cheng, L. Wang, X. Jing, F. Wang, *Adv. Funct. Mater.* **2009**, *19*, 84.
- [S3] a) C. Adachi, M. A. Baldo, M. E. Thompson, S. R. Forrest, *J. Appl. Phys.* **2001**, *90*, 5048; b) R. J. Homes, S. R. Forrest, Y.-J. Tung, R. C. Kwong, J. J. Brown, S. Garon, M. E. Thompson, *Appl. Phys. Lett.* **2003**, *82*, 2422.
- [S4] a) E. B. Namdas, A. Ruseckas, I. D. W. Samuel, S.-C. Lo, P. L. Burn, *J. Phys. Chem. B* **2004**, *108*, 1570; b) N. R. Evans, L. S. Devi, C. S. K. Mak, S. E. Watkins, S. I. Pascu, A. Koehler, R. H. Friend, C. K. Williams, A. B. Holmes, *J. Am. Chem. Soc.* **2006**, *128*, 6647; c) K. Zhang, Z. Chen, Y. Zou, S. Gong, C. Yang, J. Qin, Y. Cao, *Chem. Mater.* **2009**, *21*, 3306.
- [S5] M. Uchida, C. Adachi, T. Koyama, Y. Taniguchi, *J. Appl. Phys.* **1999**, *86*, 1680.
- [S6] a) M. Gather, R. Alle, H. Becker, K. Meerholz, *Adv. Mater.* 2007, *19*, 4460; b) S. L. M. Van Mensfoort, M. Carvelli, M. Megens, D. Wehenkel, M. Bartyzel, H. Greiner, R. A. J. Janssen, R. Coehoorn, *Nat. Photonics* 2010, *4*, 329; c) S.K. So, W. K. Choi, L. M. Leung, K. Neyts, *Appl. Phys. Lett.* 1999, *74*, 1939; d) J. -S. Kim, P. H. Ho, N. Greenham, R. Friend, *J. Appl. Phys.* 2000, *88*, 1073.
- [S7] M. S. Liu, Y.-H. Niu, J.-W. Ka, H.-L. Yip, F. Huang, J. Luo, T.-D. Kim, A. K. Y. Jen, *Macromolecules* **2008**, *41*, 9570.

[S8] S. Gong, Q. Fu, Q. Wang, C. Yang, C. Zhong, J. Qin, D. Ma, *Adv. Mater.* **2011**, 23, 4956.

[S9] W. Jiang, L. Duan, J. Qiao, G. Dong, D. Zhang, L. Wang, Y. Qiu, *J. Mater. Chem.* **2011**, 21, 4918.

[S10] K. S. Yook, J. Y. Lee, *Org. Electron.* **2011**, 12, 1711.

[S11] B. Zhang, G. Tan, C.-S. Lam, B. Yao, C.-L. Ho, L. Liu, Z. Xie, W.-Y. Wong, J. Ding, L. Wang, *Adv. Mater.* **2012**, 24, 1873.